Liquid−Liquid Equilibrium in Mixtures of the Ionic Liquid 1-*n*-Butyl-3-methylimidazolium Hexafluorophosphate and an Alkanol†

Katya Sahandzhieva, Dirk Tuma, Silke Breyer, Álvaro Pérez-Salado Kamps, and Gerd Maurer*

Chair of Applied Thermodynamics, University of Kaiserslautern, D-67653 Kaiserslautern, Germany

The liquid−liquid phase equilibrium of mixtures of the room temperature ionic liquid 1-*n*-butyl-3-methylimidazolium hexafluorophosphate, [bmim][PF_6], and three single alkanols (ethanol, 1-propanol, and 1-butanol) was investigated over the entire composition range at ambient pressure. The experiments were conducted from 262 K to the vicinity of the critical solution temperature of the binary mixture (at maximum 362 K) by two different methods, namely, synthetic cloud-point measurements and analytical UV spectroscopy. The cloud-point method was mainly applied for the [bmim][PF_6]-rich liquid, whereas UV spectroscopy was used to determine the very small concentrations of [bmim][PF_6] in the alkanols, since under these conditions the cloud-point method is no longer applicable. All three systems show an upper critical solution temperature. With increasing chain length of the alcohol, that temperature rises and simultaneously the biphasic region becomes larger. Inspired by recent publications, the liquid−liquid equilibrium of these three binary systems was predicted by applying the COSMO-RS method. Calculations resulted in predictions of a miscibility gap, but the calculated miscibility gap strongly differs from the experimental results. A far better representation of the experimental data was accomplished via a UNIQUAC-based correlation.

Introduction

The novel and successful introduction of industrial processes where an ionic liquid is formed during an acid scavenging step[1,2] opens up new prospects for the application of ionic liquids. When an ionic liquid is formed during that particular step, conditions can be set to separate it as a clear liquid phase from the product, avoiding an inconvenient salt suspension. If a process for acid scavenging that works without producing solids becomes viable, it will certainly rule out similar processes that produce solid waste, especially on a larger, industrial scale. The only thermodynamic premise is the existence of a liquid−liquid equilibrium. But before such a process can be put into operation, of course, reliable data for the encountered thermodynamic properties are required.

The existence of partial miscibility in the binary ionic liquid + alkanol system has opened the door to the application of ionic liquids in liquid−liquid separation and extraction. Which ionic liquid and which alkanol would make for the ideal combination? 1-*n*-Butyl-3-methylimidazolium hexafluorophosphate [bmim][PF_6] is the first ionic liquid subjected to systematic investigations of its thermophysical properties. However, [bmim][PF_6] is nowadays outdated as it is less stable than previously assumed.[3] Nevertheless, it may further serve as a model substance for developing and testing thermodynamic models. Since a considerable data pool on liquid−liquid phase behavior of this particular substance with alcohols is available,[4−12] we investigated the liquid−liquid equilibrium for [bmim][PF_6] in different alkanols at atmospheric pressure and different temperatures to test/confirm that data.

The knowledge of mutual solubility of ionic liquids especially with alcohols is of great importance. Generally, in a binary ionic liquid + alkanol extraction system, varying the alkanol can result in a significantly different phase behavior. On the other hand, a different ionic liquid, however, can assert a higher toxicity risk. For example, a trend of increasing toxicity with increasing alkyl chain length was observed.[13]

The IL-rich branch of the binodal curve determines the solubility of reactants or products in the ionic liquid, whereas the solvent-rich branch determines the amount of ionic liquid in the organic phase that has to be recovered. One striking characteristic of the data available so far is that there are only very few data published for the solubility of an ionic liquid in an organic solvent, in particular for systems where that solubility is small. This is also because under these conditions the synthetic cloud-point method becomes increasingly inaccurate. As the $[bmim]^+$ cation reveals UV activity, UV spectroscopy was applied in the present work to determine the concentration of the ionic liquid in the solvent-rich phase, particularly in those regions where the cloud-point method fails.

Additionally, the experimentally obtained liquid−liquid equilibrium data were compared to predictions from the COSMO-therm software package. That software package is based on quantum chemical methods and allows us to predict thermophysical properties.[14,15] Recently, the improved performance and the enlarged applicability of quantum chemical calculations resulted in many applications in the field of chemical engineering.[16,17] Ideally, the employment of packages such as COSMO-therm shall help to substitute experiments, preferably those which are time-consuming and expensive. Since most ionic liquids are still rather expensive (notably high-purity ionic liquids), such calculations can serve at least for screening various ionic liquids for their ability to be employed in applications. Ultimately, we also employed the classical UNIQUAC-G^E approach of Abrams and Prausnitz[18] to correlate the experimental results for the liquid−liquid equilibrium.

† This work was presented at the meeting Green Solvents for Synthesis, held in Bruchsal, Germany, October 3−6, 2004.

* Corresponding author. Phone: +49 631 205 2410. Fax: +49 631 205 3835. E-mail: gmaurer@rhrk.uni-kl.de.

10.1021/je050474j CCC: $30.25
Published on Web 07/06/2006

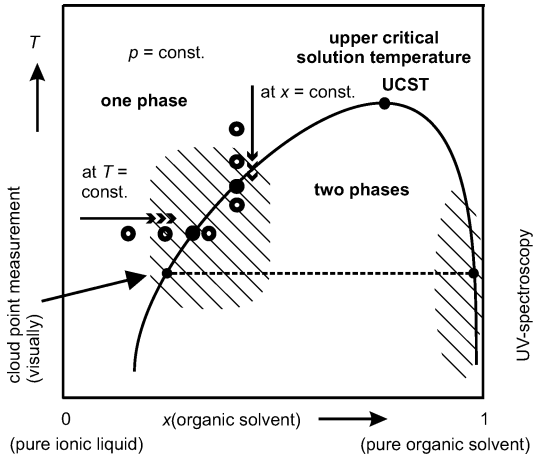

Figure 1. Typical (T, x) phase diagram for systems ionic liquid + alkanol showing an upper critical solution temperature (UCST).

Experimental Investigation of the Liquid−Liquid Phase Equilibrium

Among the variety of methods to determine the liquid−liquid equilibrium of a mixture (to map the binodal curve onto a temperature versus composition diagram) the visual "cloud-point method" is one of the most simple while also most reliable ones. In such investigations, the cloud point determines the transition from a single-phase to a two-phase system (or vice versa). That transition is either observed visually or, for example, by optical light scattering devices. At the transition from a homogeneous to a heterogeneous phase the solution becomes turbid. The two ways that are usually applied in that method are illustrated in Figure 1: either the stepwise addition of defined portions of one component (always followed by vigorous mixing) at constant temperature until the liquid stays cloudy or slowly changing the temperature of a homogeneous mixture of known composition until the cloud point is reached.

The particular advantages of that method for the systems investigated here are as follows. The large differences in the densities of the ionic liquid [bmim][PF_6] (1.37 kg·dm^{-3} at T = 297.7 K)[19] and an alkanol (from 0.79 kg·dm^{-3} for ethanol to 0.81 kg·dm^{-3} for 1-butanol at around room temperature) lead to a fast and well-defined phase separation. The cloud-point method allows the detection of the phase boundary directly without any calibration. The method can be realized in a rather simple equipment, for example, as a small thermostated glass cell connected with a thermostat and a stirring option, together with an analytical precision balance. Although rather often some optical equipment is used to detect the light scattering,[20] in most cases the human eye is well-suited to detect the cloud point. The accuracy depends on the uncertainty the masses of liquids added are afflicted with, the number of additions, and the amount of substance of the last addition (i.e., the addition that induces the cloud point in the isothermal experiment), or on the accuracy of temperature determination when the composition is fixed and the temperature varied. When the binodal curve extends to one (or both) of the pure components (cf. Figure 1), the cloud-point method becomes impracticable. Here, this happens at low temperatures where one of the coexisting liquids consists of almost the pure alkanol. Then the cloud-point method is confronted with an outsized error margin that is related to the disproportionate ratio between solvent and ionic liquid (at T = constant) or the very steep slope of the binodal (at x = constant). A stepwise addition of ionic liquid in an isothermal experiment, for example, by a microsyringe, will hardly be possible with sufficient accuracy. Furthermore, the typically high density and high viscosity of an ionic liquid also hampers the handling of such small amounts of ionic liquid. For these reasons, we employed an analytical method. The imidazolium ring of the ionic liquid [bmim][PF_6] is UV active and shows a maximum absorbance at 213 nm both in alkanols and in water.[21,22] The proposed cutoff for analytical UV spectroscopy in alkanols is located at approximately this wavelength (210 nm for ethanol, 210 nm for 1-propanol, 215 nm for 1-butanol, and 185 nm for water). These circumstances allow us to record the UV spectra of solutions of [bmim][PF_6] with known composition in these solvents in calibration experiments and to establish a reliable correlation between the maximum absorptivity (or peak area within a defined wavelength range) and the concentration of the ionic liquid. A problem might arise when the solubility is extremely small. However, then it is often possible to take another, better solvent as long as the molar absorption coefficients of the solute in both solvents do not differ significantly. In supercritical fluid spectroscopy, for example, hexane was used as a "reference solvent" for CO_2,[23] which means solubility of a UV/VIS-active substance in supercritical CO_2 can be analyzed via a calibration where the solute is dissolved in liquid hexane.

However, this method is more susceptible to the propagation of experimental errors than the cloud-point method. First, the calibration requires several stock solutions where small quantities of ionic liquid are dissolved in a rather large amount of solvent. Second, a series of UV spectra must be recorded for each sample and the peaks analyzed. The spectral analysis is done at room temperature. Consequently, when taking the sample from the biphasic mixture, it is necessary to dilute it with the pure solvent to ensure a homogeneous phase as well as to remain within the detection range of the spectrophotometer.

Materials and Methods

The ionic liquid [bmim][PF_6] ($C_8H_{15}F_6PN_2$, M = 284.18 g·mol^{-1}, purissimum, mass fraction ≥ 99 %) was supplied by Solvent Innovation GmbH, Cologne, Germany. Prior to the experiment, the samples were degassed and dried under vacuum in the same way as described previously for gas solubility experiments.[19] The water content of the ionic liquid was frequently determined by Karl Fischer titration using a Metrohm 701 KF Titrino (Deutsche Metrohm GmbH & Co. KG, Filderstadt, Germany) titrator. Before being dried, the water mass fraction of the [bmim][PF_6] samples was as large as 0.65 %. It was reduced in the drying step to about 0.04 %. That water mass fraction is compared with the water content of samples investigated by other authors. Rogers and co-workers reported a water mass fraction of 0.059 % for dried [bmim][PF_6].[4,5,24] Marsh and co-workers[6,8] estimated the water mass fraction of their ionic liquid samples (from NMR and mass spectroscopy) to 0.01 %. Najdanovic-Visak et al.[7,10] also applied NMR analysis and reported a water mass fraction of 0.15 %.

The alkanol samples of the present work were of "pro analysi" quality. They were used as supplied by Carl Roth GmbH, Karlsruhe, Germany (ethanol, mass fraction ≥ 99.8 %, water mass fraction < 0.1 %); by Merck KGaA, Darmstadt, Germany (1-propanol, mass fraction ≥ 99.5 %, water mass fraction < 0.05 %); and by Riedel-de Haën GmbH, Seelze, Germany (1-butanol, mass fraction ≥ 99.5 %, water mass fraction < 0.1 %).

Cloud-Point Method. Vials of 13 mL were half-filled with known amounts of either the ionic liquid (1) or the alkanol (2) at room temperature. They were closed by a screw cap with a Teflon sealing inside. The vials were immersed in a temperature-controlled water bath equipped with a turnover mixing device

at preset temperature. The temperature was monitored by platinum resistance thermometers (Conatex Pt100/B/4, L. Colbus GmbH, St. Wendel, Germany, with an uncertainty below ± 0.1 K). The cloud points were determined visually after adding stepwise small portions of either ionic liquid or alkanol at constant temperature by a microsyringe. The syringe was weighed before and after the addition to determine the mass of the portions (Mettler Toledo PR2003 Comparator, Mettler Toledo GmbH, Giessen, Germany). The amount of mass of an addition was usually between (0.01 and 2.5) g. After each addition, the vials were carefully shaken and placed back into the thermostat for about (15 to 20) min. When the sample was judged to be turbid the vial was shortly removed from the thermostat (for a few seconds at most) for visual inspection. The size of the last portion that induces the phase split also determines the uncertainty of the experimental results for the composition of the coexisting liquid mixture. To determine the cloud point more accurately, the experiment was repeated but started with a mixture already close to the phase boundary and reducing the amounts of mass added. After such an experiment was completed, the turbid mixture was heated to a somewhat higher temperature, and the procedure (addition of more substance) was started again (cf. Figure 1).

There are mainly two types of experimental uncertainties: The uncertainty for the mole fraction of the added solute and the uncertainty for the cloud-point temperature. The experimental uncertainty for the mole fraction of the added solute is estimated from two contributions, namely, the accumulated weighing error caused by the number of mass portions and the tolerance limit for accurate determination of turbidity. For the system ([bmim][PF_6] + ethanol), the average absolute (and relative) uncertainties for the mole fraction of the alkanol in the ionic liquid-rich phase (Δx_2 and $\Delta x_2/x_2$, respectively) and for the mole fraction of the ionic liquid in the alkanol-rich phase (Δx_1 and $\Delta x_1/x_1$, respectively) amount to 0.0038 (0.7 %) and 0.0008 (8.7 %), respectively. For the system ([bmim][PF_6] + 1-propanol), those uncertainties amount to 0.0022 (0.5 %) and 0.0011 (8.2 %), respectively. For the system ([bmim][PF_6] + 1-butanol), those uncertainties amount to 0.0017 (0.7 %) and 0.0003 (2.3 %), respectively. The uncertainty for the cloud-point temperature is estimated from the uncertainty of measuring the temperature (± 0.1 K) and the effect of traces of water in the ionic liquid and the alkanol. This latter uncertainty was estimated from the known water mass fractions of the substances (as given before) and experimental data by Heintz et al.[25] on the influence of water on the liquid−liquid equilibrium of systems of (ionic liquid + alkanol). It is assumed that for the investigations of the present work this uncertainty is well below 1 K. The overall experimental uncertainty for the cloud-point temperature is therefore estimated not to surmount ± 1 K.

UV Spectroscopy. UV spectroscopy was mainly applied to determine the mole fraction of [bmim][PF_6] in the alkanol-rich liquid mixture that coexists with an ionic liquid-rich solution. For such an analysis, about (15 to 20) mL of a biphasic mixture (containing a mole fraction of about 5 % of the ionic liquid) was equilibrated in a vial in a temperature-controlled thermostated bath (thermostat: Lauda RSC6, Lauda Dr. R. Wobser GmbH & Co. KG, Lauda-Königshofen, Germany). The vial was sealed with a glass plug through which a platinum resistance thermometer (Conatex Pt100/B/4) was immersed in the sample for temperature measurement. The vessel also contained a Teflon-coated magnetic rod to enable stirring. After equilibration and phase separation were completed, a sample was pipetted from the alkanol-rich phase and instantaneously dispensed into a vial that already contained a known amount of the alkanol. When working at temperatures above room temperature, the pipet was preheated to avoid a phase split. The sample size was between (0.05 and 0.6) mL, and the volume of diluting solvent was allotted between (10 and 15) mL. The masses of both the sample and the diluent were determined by a high-precision balance (Mettler Toledo AE 240). A quartz cuvette (path length 10 mm) was filled with the diluted alkanol-rich phase, and the UV spectrum was recorded between (185 and 350) nm with a double-beam, double-monochromator UV/VIS spectrophotometer (Perkin-Elmer Lambda 18, Perkin-Elmer Life and Analytical Sciences, Inc., Wellesley, MA). The reference cuvette was filled with the respective alkanol. The area of the peak half covering the wavelength distance from the absorption maximum (213 nm for ethanol and 1-propanol and 212 nm for 1-butanol) to 240 nm was taken for the composition analysis. Prior to the measurement, calibration experiments were performed. The UV spectra of [bmim][PF_6] in the three alkanols are almost equal, but ethanol is by far the best solvent. Due to the extremely poor solubility of [bmim][PF_6] in 1-propanol and 1-butanol, ethanol was always used as the solvent in the calibration procedure. The average absolute and relative uncertainties for the mole fraction of the ionic liquid in the alkanol-rich phase (Δx_1 and $\Delta x_1/x_1$, respectively) were calculated from the standard deviation for the calibration curve in the spectrophotometric analysis and amount to 0.0015 (16.3 %) for the system ([bmim][PF_6] + ethanol), 0.0002 (15.4 %) for the system ([bmim][PF_6] + 1-propanol), and 0.0002 (15.3 %) for the system ([bmim][PF_6] + 1-butanol). The overall experimental uncertainty for the demixing temperature is adherent to the water content and estimated to be ± 1 K at the utmost (see previous section). A spectroscopic analysis of the ionic liquid-rich phase is possible, but due to the necessity of extreme dilution, the error becomes so high that this method was not applied here.

Results and Discussion

Liquid−Liquid Equilibrium Measurements. The experimental results for the binodal curves of the three binary systems {[bmim][PF_6] + (ethanol or 1-propanol or 1-butanol)} are given in Tables 1 to 3 and shown in Figures 2 to 4. The liquid−liquid equilibria of all three systems investigated show the typical behavior of a partially miscible system with an upper critical solution temperature (UCST). The temperature of the UCST rises with increasing chain length of the alkanol, and simultaneously the biphasic concentration region becomes larger. Although several experiments were carried out at temperatures below the melting point of pure [bmim][PF_6] (T_{fus}([bmim][PF_6]) = 276.4 K),[26] no solid phases were observed. These findings agree with previous work by Marsh and co-workers[6,8,12] and Wagner et al.[9] (which focuses on critical points only) as well with the results published by Heintz et al.[20] and Crosthwaite et al.[27] for other binary mixtures of an ionic liquid and an alkanol. Marsh et al. found that methanol is completely miscible with [bmim][PF_6] at room temperature.[6] However, it was also observed that by pressurization with carbon dioxide a liquid mixture of ([bmim][PF_6] + methanol) can be split into two liquid phases.[28−30]

[bmim][PF_6] (1) + Ethanol (2). The new experimental results for the liquid−liquid equilibrium are compared in Figure 2 to three data sets taken from the literature.[3,4,7,10,11] The new experimental results for the composition of the ionic liquid-rich phase reveal slightly lower mole fractions of ethanol when compared with the data reported by Marsh et al.[6] and Najdanovic-Visak et al.[7,10] These two data sets, however, coincide

Table 1. Liquid−Liquid Equilibria for [bmim][PF_6] (1) + Ethanol (2) at p = 0.1 MPa[a]

	[bmim][PF_6]-rich phase			ethanol-rich phase		
T/K	$x_2 \pm \Delta x_2$	$w_2 \pm \Delta w_2$		$x_1 \pm \Delta x_1$	$w_1 \pm \Delta w_1$	
288.2	0.4835 ± 0.0038	0.1318 ± 0.0019	CP	0.0047 ± 0.0008	0.0285 ± 0.0021	CP
288.2	0.4789 ± 0.0038	0.1297 ± 0.0019	CP	0.0047 ± 0.0008	0.0285 ± 0.0021	CP
288.2	0.4837 ± 0.0038	0.1318 ± 0.0019	CP			
293.2	0.5048 ± 0.0038	0.1418 ± 0.0019	CP	0.0063 ± 0.0008	0.0375 ± 0.0021	CP
293.2	0.5090 ± 0.0038	0.1439 ± 0.0019	CP	0.0065 ± 0.0008	0.0389 ± 0.0021	CP
295.2	0.5180 ± 0.0038	0.1484 ± 0.0019	CP			
295.2	0.5255 ± 0.0038	0.1522 ± 0.0019	CP			
298.2	0.5489 ± 0.0038	0.1648 ± 0.0019	CP	0.0071 ± 0.0008	0.0423 ± 0.0021	CP
298.2	0.5459 ± 0.0038	0.1631 ± 0.0019	CP	0.0070 ± 0.0008	0.0416 ± 0.0021	CP
308.1	0.6320 ± 0.0038	0.2178 ± 0.0019	CP	0.0112 ± 0.0008	0.0696 ± 0.0021	CP
308.1	0.6329 ± 0.0038	0.2185 ± 0.0019	CP	0.0127 ± 0.0008	0.0737 ± 0.0021	CP
318.1	0.7149 ± 0.0038	0.2890 ± 0.0019	CP	0.0231 ± 0.0008	0.1273 ± 0.0021	CP
318.1	0.7141 ± 0.0038	0.2882 ± 0.0019	CP	0.0234 ± 0.0008	0.1288 ± 0.0021	CP
328.0	0.8279 ± 0.0038	0.4382 ± 0.0019	CP	0.0636 ± 0.0008	0.2951 ± 0.0021	CP
328.0	0.8267 ± 0.0038	0.4361 ± 0.0019	CP	0.0644 ± 0.0008	0.2982 ± 0.0021	CP
279.1				0.0041 ± 0.0007	0.0249 ± 0.0038	UV
279.1				0.0039 ± 0.0007	0.0233 ± 0.0036	UV
279.1				0.0040 ± 0.0006	0.0241 ± 0.0037	UV
279.1				0.0039 ± 0.0006	0.0234 ± 0.0036	UV
279.1				0.0037 ± 0.0006	0.0222 ± 0.0034	UV
279.1				0.0039 ± 0.0006	0.0236 ± 0.0036	UV
284.0				0.0045 ± 0.0007	0.0271 ± 0.0042	UV
284.0				0.0049 ± 0.0008	0.0297 ± 0.0046	UV
284.0				0.0046 ± 0.0007	0.0276 ± 0.0043	UV
284.0				0.0048 ± 0.0008	0.0288 ± 0.0044	UV
284.0				0.0048 ± 0.0008	0.0288 ± 0.0045	UV
284.0				0.0047 ± 0.0007	0.0283 ± 0.0044	UV
289.0				0.0056 ± 0.0009	0.0335 ± 0.0052	UV
289.0				0.0057 ± 0.0009	0.0339 ± 0.0052	UV
289.0				0.0061 ± 0.0010	0.0366 ± 0.0057	UV
289.0				0.0060 ± 0.0010	0.0358 ± 0.0055	UV
289.0				0.0060 ± 0.0010	0.0360 ± 0.0055	UV
289.0				0.0058 ± 0.0009	0.0350 ± 0.0054	UV
293.9				0.0066 ± 0.0011	0.0395 ± 0.0061	UV
293.9				0.0066 ± 0.0011	0.0392 ± 0.0060	UV
293.9				0.0068 ± 0.0011	0.0402 ± 0.0062	UV
298.8				0.0083 ± 0.0014	0.0493 ± 0.0076	UV
298.8				0.0080 ± 0.0013	0.0472 ± 0.0073	UV
298.8				0.0083 ± 0.0014	0.0492 ± 0.0076	UV
303.9				0.0099 ± 0.0016	0.0580 ± 0.0090	UV
303.9				0.0099 ± 0.0016	0.0581 ± 0.0090	UV
303.9				0.0100 ± 0.0016	0.0584 ± 0.0090	UV
308.8				0.0162 ± 0.0027	0.0919 ± 0.014	UV
308.8				0.0167 ± 0.0028	0.0949 ± 0.015	UV
308.8				0.0154 ± 0.0026	0.0881 ± 0.014	UV
308.8				0.0142 ± 0.0024	0.0817 ± 0.013	UV
308.8				0.0148 ± 0.0025	0.0846 ± 0.013	UV
308.8				0.0167 ± 0.0028	0.0947 ± 0.015	UV
308.8				0.0169 ± 0.0029	0.0960 ± 0.015	UV
308.8				0.0145 ± 0.0024	0.0831 ± 0.013	UV
308.8				0.0142 ± 0.0024	0.0816 ± 0.013	UV
313.8				0.0190 ± 0.0033	0.1069 ± 0.016	UV
313.8				0.0197 ± 0.0034	0.1101 ± 0.017	UV
313.8				0.0189 ± 0.0033	0.1061 ± 0.016	UV

[a] x_i represents the mole fraction. w_i represents the mass fraction of the solvent.

very well. In the temperature interval between (288 and 320) K, the average absolute and relative deviation (Δx_2 and $\Delta x_2/x_2$, respectively) between our and Marsh's data amount to 0.020 (3.4 %). Only Marsh et al.[6] reported experimental results at higher temperatures. While the discrepancy between the new results and those by Marsh et al.[6] decrease toward lower temperatures, the deviation becomes larger in the vicinity of the UCST. From the new results, the critical temperature is estimated (from the UNIQUAC correlation; cf. the following section) to be at approximately 330 K, whereas both other data sets indicate that temperature to be about 325 K. Crosthwaite et al.[27] assumed that already small contaminations of water shift the UCST to lower temperatures. Heintz et al.[25] supported that finding.

The solubility of [bmim][PF_6] (1) in ethanol (2) is much smaller than the solubility of ethanol in [bmim][PF_6]; for example, at 300 K $x_1 \approx 0.009$ whereas $x_2 \approx 0.56$. Therefore, two different composition scales are used in Figure 2 (as well as in Figures 3 and 4). The mole fraction of the ionic liquid in ethanol reported by Najdanovic-Visak et al.[7,10] at T = 298.6 K differs from the new experimental results by the UV method (at T = 298.8 K) by $\Delta x_1 = 0.0001$ ($\Delta x_1/x_1 = 1.2$ %). Looking in the same way at the data of Marsh et al.[6] gives $\Delta x_1 = 0.0014$ ($\Delta x_1/x_1 = 26.2$ %) at T = 291.0 K and $\Delta x_1 = 0.0007$ ($\Delta x_1/x_1 = 4.4$ %) at T = 310.5 K.

[bmim][PF_6] (1) + 1-Propanol (2). The new experimental data for the liquid−liquid equilibrium are shown in Figure 3 for comparison with the data reported by Marsh et al.[6] The

Table 2. Liquid−Liquid Equilibria for [bmim][PF_6] (1) + 1-propanol (2) at p = 0.1 MPa[a]

	[bmim][PF_6]-rich phase			1-propanol-rich phase		
T/K	$x_2 \pm \Delta x_2$	$w_2 \pm \Delta w_2$		$x_1 \pm \Delta x_1$	$w_1 \pm \Delta w_1$	
293.2	0.2755 ± 0.0022	0.0744 ± 0.0020	CP			
293.2	0.2721 ± 0.0022	0.0732 ± 0.0020	CP			
303.2	0.3285 ± 0.0022	0.0938 ± 0.0020	CP			
303.2	0.3293 ± 0.0022	0.0941 ± 0.0020	CP			
313.1	0.3838 ± 0.0022	0.1164 ± 0.0020	CP			
313.1	0.3831 ± 0.0022	0.1161 ± 0.0020	CP			
323.1	0.4517 ± 0.0022	0.1484 ± 0.0020	CP			
323.1	0.4508 ± 0.0022	0.1479 ± 0.0020	CP			
333.0	0.5279 ± 0.0022	0.1912 ± 0.0020	CP	0.0076 ± 0.0011	0.0349 ± 0.0045	CP
333.0	0.5243 ± 0.0022	0.1890 ± 0.0020	CP	0.0084 ± 0.0011	0.0384 ± 0.0045	CP
343.0	0.6006 ± 0.0022	0.2413 ± 0.0020	CP	0.0147 ± 0.0011	0.0660 ± 0.0045	CP
343.0	0.5992 ± 0.0022	0.2402 ± 0.0020	CP	0.0169 ± 0.0011	0.0751 ± 0.0045	CP
352.4	0.6439 ± 0.0022	0.2766 ± 0.0020	CP	0.0288 ± 0.0011	0.1230 ± 0.0045	CP
352.4	0.6483 ± 0.0022	0.2805 ± 0.0020	CP	0.0297 ± 0.0011	0.1262 ± 0.0045	CP
361.9	0.7498 ± 0.0022	0.3879 ± 0.0020	CP			
361.9	0.7520 ± 0.0022	0.3907 ± 0.0020	CP			
262.6				0.0004 ± 0.0001	0.0020 ± 0.0003	UV
262.6				0.0004 ± 0.0001	0.0020 ± 0.0003	UV
262.6				0.0004 ± 0.0001	0.0020 ± 0.0003	UV
267.6				0.0006 ± 0.0001	0.0029 ± 0.0004	UV
267.6				0.0005 ± 0.0001	0.0026 ± 0.0004	UV
267.6				0.0005 ± 0.0001	0.0026 ± 0.0004	UV
271.4				0.0007 ± 0.0001	0.0031 ± 0.0005	UV
271.4				0.0006 ± 0.0001	0.0030 ± 0.0005	UV
271.4				0.0006 ± 0.0001	0.0030 ± 0.0005	UV
274.3				0.0007 ± 0.0001	0.0035 ± 0.0005	UV
274.3				0.0007 ± 0.0001	0.0033 ± 0.0005	UV
274.3				0.0007 ± 0.0001	0.0034 ± 0.0005	UV
278.2				0.0008 ± 0.0001	0.0036 ± 0.0006	UV
278.2				0.0008 ± 0.0001	0.0037 ± 0.0006	UV
278.2				0.0007 ± 0.0001	0.0034 ± 0.0005	UV
284.1				0.0009 ± 0.0002	0.0045 ± 0.0007	UV
284.1				0.0009 ± 0.0002	0.0044 ± 0.0007	UV
284.1				0.0009 ± 0.0001	0.0044 ± 0.0007	UV
289.0				0.0012 ± 0.0002	0.0055 ± 0.0009	UV
289.0				0.0012 ± 0.0002	0.0055 ± 0.0009	UV
289.0				0.0012 ± 0.0002	0.0056 ± 0.0009	UV
294.0				0.0016 ± 0.0002	0.0074 ± 0.0011	UV
294.0				0.0015 ± 0.0002	0.0068 ± 0.0011	UV
294.0				0.0014 ± 0.0002	0.0068 ± 0.0010	UV
298.9				0.0019 ± 0.0003	0.0088 ± 0.0014	UV
298.9				0.0019 ± 0.0003	0.0088 ± 0.0014	UV
298.9				0.0019 ± 0.0003	0.0088 ± 0.0014	UV
303.9				0.0023 ± 0.0004	0.0107 ± 0.0016	UV
303.9				0.0023 ± 0.0004	0.0110 ± 0.0017	UV
303.9				0.0023 ± 0.0004	0.0108 ± 0.0017	UV
308.8				0.0025 ± 0.0004	0.0117 ± 0.0018	UV
308.8				0.0026 ± 0.0004	0.0122 ± 0.0019	UV
308.8				0.0026 ± 0.0004	0.0122 ± 0.0019	UV
313.8				0.0032 ± 0.0005	0.0151 ± 0.0023	UV
313.8				0.0031 ± 0.0005	0.0145 ± 0.0022	UV
313.8				0.0033 ± 0.0005	0.0152 ± 0.0024	UV

[a] x_i represents the mole fraction. w_i represents the mass fraction of the solvent.

differences between both data sets are very similar to those described before with ethanol (instead of 1-propanol). However, the discrepancies are larger in particular for the composition of the [bmim][PF_6]-rich phase and the coordinates of the critical point. Within the temperature range from (293.2 to 352.4) K, the absolute (and the relative) difference Δx_2 (and $\Delta x_2/x_2$) for the mole fraction of 1-propanol in the [bmim][PF_6]-rich phase increases from 0.018 to 0.122 (and from 6.3 % to 19.0 %). A similar analysis for the difference in the mole fraction of [bmim][PF_6] in the propanol-rich liquid phase (Δx_1 and $\Delta x_1/x_1$, respectively) between both data sets results in 0.0002 (1.3 %) at 343 K and 0.0003 (0.9 %) at 352 K. The correlation of the new experimental results by the UNIQUAC equation yields the critical point at T(UCST) = 368 K and x_2 = 0.90, whereas Marsh et al. reported (357 ± 0.2) K at x_2 = 0.92.[6]

[bmim][PF$_6$] (1) + 1-Butanol (2). Figure 4 shows a comparison between the data of Marsh and co-workers[6,8] and the results of the present work. That comparison reveals somewhat larger differences as those observed in the systems discussed above especially for the ionic liquid-rich phase. It can also be seen that the new data for this system are afflicted by a larger scattering. The average absolute (Δx_2) and relative ($\Delta x_2/x_2$) differences amount to 0.068 and 20.2 %, respectively, in the temperature interval between (298 and 362) K. The relative deviation for the mole fraction of [bmim][PF_6] in the butanol-rich liquid phase is $\Delta x_1/x_1$ = 9.9 % at T = 369.0 K. As the liquid−liquid miscibility gap extends far beyond the maximum temperature of the present work, no attempt was made to extrapolate the new results up to the UCST—but the new results indicate that the two-phase region extends beyond the

Table 3. Liquid−Liquid Equilibria for [bmim][PF_6] (1) + 1-Butanol (2) at $p = 0.1$ MPa[a]

	[bmim][PF_6]-rich phase			1-butanol-rich phase		
T/K	$x_2 \pm \Delta x_2$	$w_2 \pm \Delta w_2$		$x_1 \pm \Delta x_1$	$w_1 \pm \Delta w_1$	
283.2	0.1371 ± 0.0017	0.0398 ± 0.0006	CP			
283.2	0.1404 ± 0.0017	0.0409 ± 0.0006	CP			
288.2	0.1621 ± 0.0017	0.0480 ± 0.0006	CP			
288.2	0.1600 ± 0.0017	0.0473 ± 0.0006	CP			
291.2	0.1686 ± 0.0017	0.0502 ± 0.0006	CP			
291.2	0.1670 ± 0.0017	0.0497 ± 0.0006	CP			
293.2	0.1779 ± 0.0017	0.0534 ± 0.0006	CP			
293.2	0.1755 ± 0.0017	0.0526 ± 0.0006	CP			
298.2	0.2107 ± 0.0017	0.0651 ± 0.0006	CP			
298.2	0.2108 ± 0.0017	0.0651 ± 0.0006	CP			
308.1	0.2357 ± 0.0017	0.0745 ± 0.0006	CP			
308.1	0.2352 ± 0.0017	0.0743 ± 0.0006	CP			
318.1	0.3038 ± 0.0017	0.1022 ± 0.0006	CP			
318.1	0.3036 ± 0.0017	0.1021 ± 0.0006	CP			
333.0	0.3509 ± 0.0017	0.1236 ± 0.0006	CP			
333.0	0.3514 ± 0.0017	0.1238 ± 0.0006	CP			
347.2	0.4088 ± 0.0017	0.1528 ± 0.0006	CP			
347.2	0.4094 ± 0.0017	0.1531 ± 0.0006	CP			
357.1	0.4447 ± 0.0017	0.1728 ± 0.0006	CP			
357.1	0.4438 ± 0.0017	0.1722 ± 0.0006	CP			
361.9	0.4876 ± 0.0017	0.1989 ± 0.0006	CP	0.0127 ± 0.0003	0.0469 ± 0.0010	CP
361.9	0.4868 ± 0.0017	0.1983 ± 0.0006	CP	0.0131 ± 0.0003	0.0485 ± 0.0010	CP
278.2				0.0004 ± 0.0001	0.0016 ± 0.0002	UV
278.2				0.0004 ± 0.0001	0.0015 ± 0.0002	UV
278.2				0.0004 ± 0.0001	0.0016 ± 0.0002	UV
281.1				0.0005 ± 0.0001	0.0017 ± 0.0003	UV
281.1				0.0005 ± 0.0001	0.0018 ± 0.0003	UV
281.1				0.0005 ± 0.0001	0.0018 ± 0.0003	UV
284.1				0.0004 ± 0.0001	0.0017 ± 0.0003	UV
284.1				0.0004 ± 0.0001	0.0017 ± 0.0003	UV
284.1				0.0004 ± 0.0001	0.0017 ± 0.0003	UV
289.0				0.0005 ± 0.0001	0.0020 ± 0.0003	UV
289.0				0.0005 ± 0.0001	0.0020 ± 0.0003	UV
289.0				0.0005 ± 0.0001	0.0020 ± 0.0003	UV
293.9				0.0007 ± 0.0001	0.0025 ± 0.0004	UV
293.9				0.0007 ± 0.0001	0.0025 ± 0.0004	UV
293.9				0.0007 ± 0.0001	0.0025 ± 0.0004	UV
298.9				0.0008 ± 0.0001	0.0030 ± 0.0005	UV
298.9				0.0008 ± 0.0001	0.0030 ± 0.0005	UV
298.9				0.0008 ± 0.0001	0.0030 ± 0.0005	UV
303.8				0.0011 ± 0.0002	0.0040 ± 0.0006	UV
303.8				0.0011 ± 0.0002	0.0041 ± 0.0006	UV
303.8				0.0010 ± 0.0002	0.0040 ± 0.0006	UV
308.8				0.0012 ± 0.0002	0.0045 ± 0.0007	UV
308.8				0.0012 ± 0.0002	0.0046 ± 0.0007	UV
308.8				0.0012 ± 0.0002	0.0045 ± 0.0007	UV
313.8				0.0016 ± 0.0002	0.0060 ± 0.0009	UV
313.8				0.0016 ± 0.0002	0.0059 ± 0.0009	UV
313.8				0.0016 ± 0.0002	0.0060 ± 0.0009	UV
323.7				0.0024 ± 0.0004	0.0091 ± 0.0014	UV
323.7				0.0024 ± 0.0004	0.0093 ± 0.0014	UV
323.7				0.0024 ± 0.0004	0.0092 ± 0.0014	UV
333.7				0.0040 ± 0.0006	0.0150 ± 0.0023	UV
333.7				0.0039 ± 0.0006	0.0148 ± 0.0023	UV
333.7				0.0038 ± 0.0006	0.0146 ± 0.0023	UV
333.7				0.0038 ± 0.0006	0.0144 ± 0.0022	UV

[a] x_i represents the mole fraction. w_i represents the mass fraction of the solvent.

critical temperature reported by Wu et al.[8] {T(UCST) = 376 K}.

Modeling

Correlation by Means of the UNIQUAC Equation. The experimental results were correlated applying the UNIQUAC equation of Abrams and Prausnitz[18] for the Gibbs excess energy. For the sake of simplicity, the ionic liquid [bmim][PF_6] was treated as a single neutral component and the alcohols as nonassociating substances. Due to these assumptions, the results are considered as a correlation that might serve for interpolation purposes. The chemical potential of a component was normalized according to Raoult's law (i.e., the reference state is the pure liquid at equilibrium temperature). As usual, the influence of pressure on the liquid−liquid equilibrium was neglected. Applying UNIQUAC requires the number of nearest neighbors (or coordination number), which was set at $z = 10$ as usual. The pure component UNIQUAC size (r_i) and surface parameters (q_i) were estimated according to Bondi[31] (for the alkanols and the $[bmim]^+$ ion) or adopted (for the $[PF_6]^-$ ion) from the ionic radii reported by Marcus.[32] The two binary UNIQUAC parameters for interactions between different molecules ($\psi_{i,j}$) were assumed to depend on temperature through

$$\psi_{i,j} = \exp\left[-\left(a_{i,j} + \frac{b_{i,j}}{(T/K)}\right)\right] \quad (1)$$

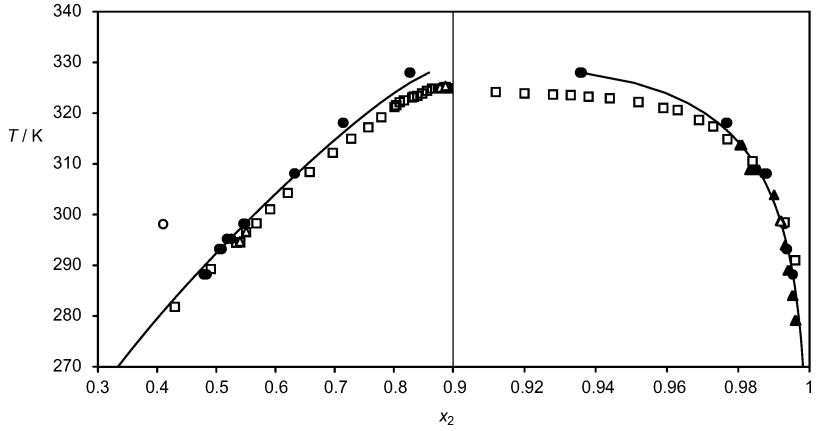

Figure 2. Liquid−liquid (T, x) phase diagram of {[bmim][PF_6] (1) + ethanol (2)}. The solvent-rich branch of the binodal (right diagram) is given in zoomed view. ●, cloud-point measurement; ▲, UV spectroscopy; ○, refs 4 and 5; □, ref 6; △, refs 7 and 10; —, UNIQUAC correlation.

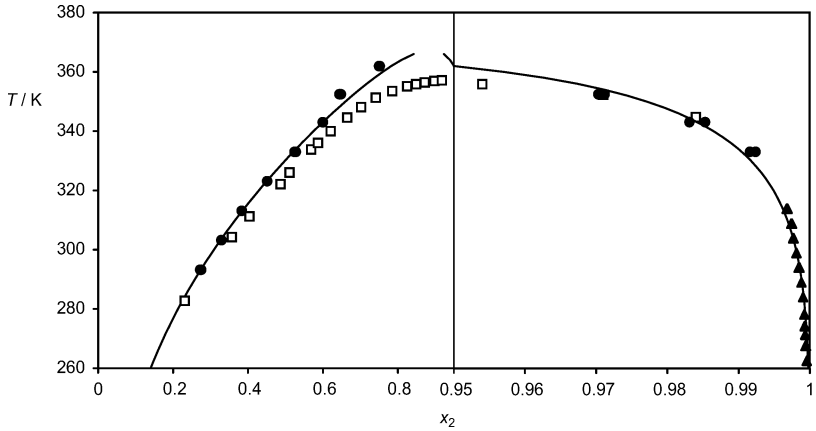

Figure 3. Liquid−liquid (T, x) phase diagram of {[bmim][PF_6] (1) + 1-propanol (2)}. The solvent-rich branch of the binodal (right diagram) is given in zoomed view. ●, cloud-point measurement; ▲, UV spectroscopy; □, ref 6; —, UNIQUAC correlation.

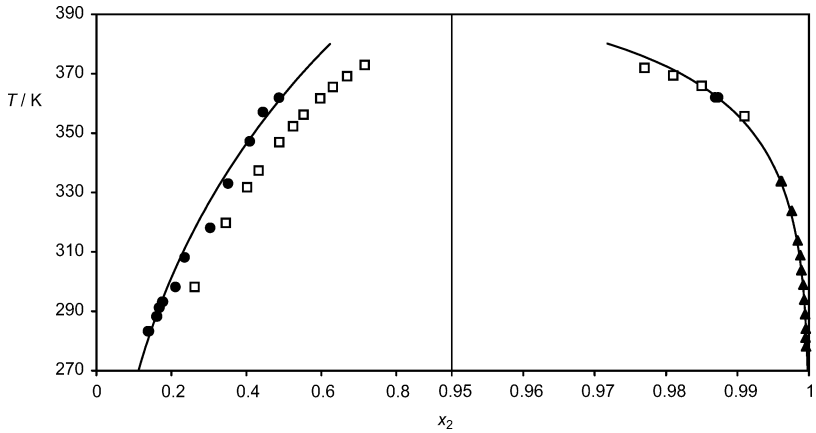

Figure 4. Liquid−liquid (T, x) phase diagram of {[bmim][PF_6] (1) + 1-butanol (2)}. The solvent-rich branch of the binodal (right diagram) is given in zoomed view. ●, cloud-point measurement; ▲, UV spectroscopy; □, refs 6 and 8; —, UNIQUAC correlation.

The four binary parameters ($a_{i,j}$, $a_{j,i}$, $b_{i,j}$, and $b_{j,i}$) were fitted to the experimental results of the present work. The respective parameters are given in Table 4.

The results of these correlations are compared to the underlying experimental data in Figures 2 to 4. The average absolute (relative) deviation between the experimental results for the mole fraction of the alkanol x_2 in the ionic liquid-rich phase amounts to 0.0117 (1.8 %) for ([bmim][PF_6] + ethanol), 0.0100 (1.6 %) for ([bmim][PF_6] + 1-propanol), and 0.0123 (4.4 %) for ([bmim][PF_6] + 1-butanol). The mean absolute (relative) deviation for the mole fraction of the ionic liquid x_1 in the alkanol-rich phase amounts to 0.0010 (12.4 %) for ([bmim][PF_6]

Table 4. UNIQUAC Size (r_i) and Surface (q_i) Parameters for the Employed Substances Together with the Adjusted Mixture Parameters $a_{i,j}$ and $b_{i,j}$

i	r_i	q_i
[bmim][PF_6]	8.5506	6.5172
ethanol	2.1055	1.9720
1-propanol	2.7799	2.5120
1-butanol	3.4543	3.0520

i	j	$a_{i,j}$	$a_{j,i}$	$b_{i,j}$	$b_{j,i}$
ethanol	[bmim][PF_6]	−0.017922	−1.8818	208.76	611.00
1-propanol	[bmim][PF_6]	−0.051762	−1.4431	292.86	455.19
1-butanol	[bmim][PF_6]	−0.048162	−1.1192	342.04	334.15

+ ethanol), 0.0004 (17.1 %) for ([bmim][PF_6] + 1-propanol), and 0.0001 (8.6 %) for ([bmim][PF_6] + 1-butanol).

Predictions from the COSMO-RS Method. Recently, quantum chemistry based models have attracted a lot of interest to predict thermodynamic properties (e.g., activity coefficients).[16] Here, the COSMO-RS method of Klamt and co-workers is tested for its ability to predict the liquid−liquid phase equilibrium of the investigated systems.[14,15] In this model, molecules in solution interact via the so-called screening charge density on their surfaces (σ), which can be obtained by quantum chemical COSMO calculations.[33] COSMO-RS allows the calculation of thermodynamic properties by using a statistical thermodynamics procedure based on interactions that are defined by the screening charge density profile (or σ-profile). A σ-profile of an individual component must be calculated only once (i.e., it is independent of the solvent mixture under consideration) and can be stored like a fingerprint in a database for further use. The σ-profile of a multicomponent system is simply the sum of the σ-profiles of the components weighted with their mole fractions in the mixture. Such σ-profiles are available for many molecular and ionic components in COSMO files, but the profiles depend on the quantum chemical approximation applied. The COSMO-RS method of Klamt and co-workers[14,15] allows the calculation of chemical potentials from the temperature and the composition of the mixture when the surface structure and the σ-profile of the individual components are known.

COSMO-RS actually does not result in the chemical potential $\mu_i(T, x_j)$ itself, but in the following related quantity:

$$\ln \phi_i(T, x_j) = \frac{\mu_i(T, x_j)}{RT} - \ln x_i \tag{2}$$

where x_i is the mole fraction of component i in the liquid mixture. Note that ϕ_i is not an activity coefficient, since it is not necessary to define a reference state for the chemical potential. No influence of pressure on the chemical potentials is taken into account by COSMO-RS.

In the following section, the theoretical background of the method and its adaptation for the calculation of liquid−liquid equilibria of systems (ionic liquid + alkanol) is outlined. A number of parameters (in total 16) are required in that calculation. Those parameters are internally implemented in the COSMO-RS software package COSMOtherm and were fitted by Klamt and co-workers to a large experimental database of various thermodynamic properties that finally appear as difference in chemical potentials at different (liquid or gaseous) reference states. Obviously, the chemical potential of a pure substance in the ideal gas state is also required in that correlation. Since the database is continuously being extended resulting in new parametrizations, calculation results obtained via COSMOtherm should always be repeated together with the respective software release numbers.

For a binary system ionic liquid + alkanol under consideration, the phase equilibrium condition for the liquid−liquid equilibrium is

$$\mu'_A = \mu''_A \tag{3}$$

$$\mu'_{MX} = \mu''_{MX} \tag{4}$$

where A and MX stand for the alkanol and the ionic liquid, respectively, and where the two liquid phases are denoted by the superscripts ′ and ″, respectively. As recommended, cation M and anion X of the ionic liquid were treated as separate species with the same mole fraction, and the ionic liquid was assumed to be completely dissociated (cf. also refs 6, 8, and 12). Therefore, our calculations were performed for a pseudo-ternary system. For each liquid phase:

$$x_A + x_M + x_X = 1 \tag{5}$$

$$x_A = \frac{n_A}{n_A + 2n_{MX}} \tag{6}$$

$$x_M = x_X = \frac{n_{MX}}{n_A + 2n_{MX}} = \frac{1 - x_A}{2} \tag{7}$$

Considering the 1:1 ionic liquid [bmim][PF_6] yields:

$$\mu_{MX} = \mu_M + \mu_X \tag{8}$$

Combining eqs 2 and 3 gives

$$\ln \phi'_A(T, x'_A) + \ln x'_A = \ln \phi''_A(T, x''_A) + \ln x''_A \tag{9}$$

Then, combining eqs 2, 4, 7, and 8 results in

$$\ln \phi'_M(T, x'_A) + \ln \phi'_X(T, x'_A) + 2 \ln(1 - x'_A) = \ln \phi''_M(T, x''_A) + \ln \phi''_X(T, x''_A) + 2 \ln(1 - x''_A) \tag{10}$$

The software package COSMOtherm in its version C2.1, release 01.04, was employed to calculate ln ϕ_i. That means that all parameters of COSMOtherm {for example, σ-profiles, number of conformers of the individual components (3 for $[bmim]^+$, 1 for $[PF_6]^-$, 2 for each of the alkanols), and weighting of the conformers} were those implemented in that release. A compiled version of this software package was provided by COSMOlogic GmbH & Co. KG, Leverkusen, Germany, and linked to our own software to solve the phase equilibrium conditions (eqs 9 and 10), resulting in the composition of the two liquid (pseudoternary) phases (for a given temperature). The stoichiometric composition of each phase was finally calculated from

$$\bar{x}_A = \frac{x_A}{x_A + x_M} = 1 - \bar{x}_{MX} \tag{11}$$

To solve the equation system, partial derivatives of ln ϕ_i with respect to the unknown variables are required. When conformers are involved in the calculations, those derivatives are not provided by COSMOtherm and had to be calculated numerically. Additionally, some calculations were performed with two previous versions of COSMOtherm (C1.2, release 05.02, and C1.2, release 01.03) to check whether different versions (i.e., different parametrizations) will provide dissenting results.

The results of the calculations for the investigated binary systems are shown together with the experimental data in Figures 5 to 7. The COSMOtherm calculations predicted the existence of a two-phase region with an UCST for all three binary systems. But Figures 5 to 7 show large quantitative differences between predicted data and the experimental results. Moreover, COSMOtherm calculations do not provide the coordinates for the UCST, since in the vicinity of the critical point the software fails. For the system {[bmim][PF_6] (1) + ethanol (2)} (Figure 5) the binodal curve is shifted to lower temperatures and to a smaller region of immiscibility. The temperature of the UCST is extremely shifted (by about 40 K), with x_2 approximately at 0.75. Both applied releases (C1.2, release 01.03, and C2.1, release 01.04) give nearly the same results. These effects are even slightly more pronounced for the latest version C2.1, release 01.04. For the system {[bmim][PF_6] (1) + 1-propanol (2)} (cf. Figure 6) both

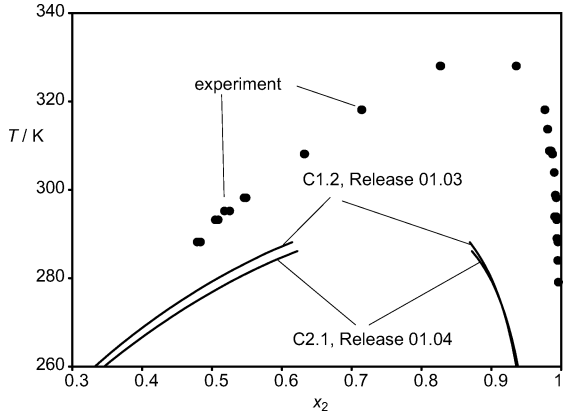

Figure 5. System {[bmim][PF_6] (1) + ethanol (2)}: Comparison of experimental liquid−liquid phase data (solid symbols) with data calculated from COSMOtherm.

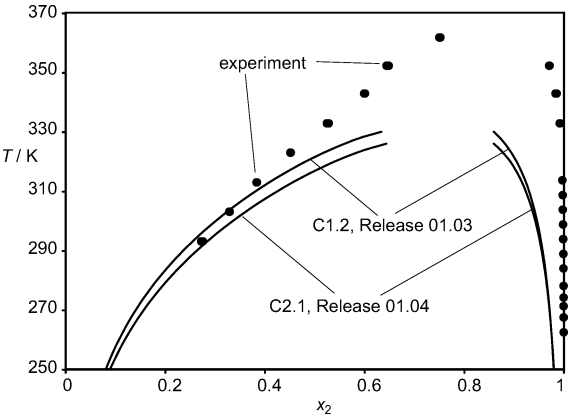

Figure 6. System {[bmim][PF_6] (1) + 1-propanol (2)}: Comparison of experimental liquid−liquid phase data (solid symbols) with data calculated from COSMOtherm.

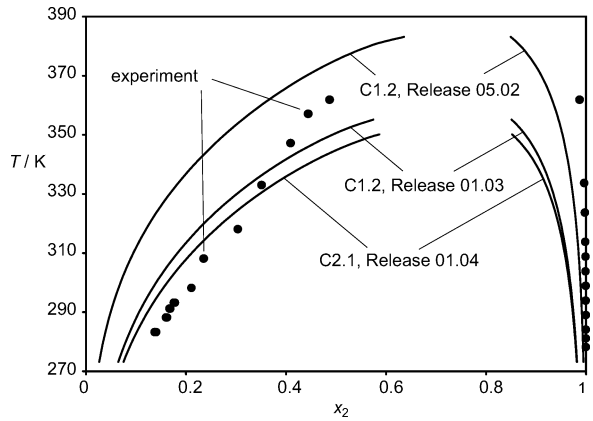

Figure 7. System {[bmim][PF_6] (1) + 1-butanol (2)}: Comparison of experimental liquid−liquid phase data (solid symbols) with data calculated from COSMOtherm.

COSMOtherm releases give a fair agreement for the composition of the [bmim][PF_6]-rich side of the binodal between approximately (280 and 315) K. However, the UCST is underestimated by about 40 K. The latest release (C2.1, release 01.04) gives slightly worse results when compared to the previous one (C1.2, release 01.03). For the system {[bmim][PF_6] (1) + 1-butanol (2)} COSMOtherm calculations were performed for three different releases (cf. Figure 7). The oldest version (C1.2, release 05.02) overestimates the two-phase region, whereas both newer releases (C1.2, release 01.03, and C2.1, release 01.04) shift the two-phase region in the direction of lower concentrations of the ionic liquid as well to lower temperatures. With all three releases the COSMOtherm calculations for the solvent-rich branch of the binodal predict a distinctly higher content of ionic liquid in the solvent phase than found experimentally. The results for the ionic liquid-rich branch of the binodal from the latest version (C2.1, release 01.04) are rather close to experimental data at temperatures from about (280 to 330) K, but the temperature of the UCST is strongly underestimated. Marsh and co-workers[6,8,12] reported COSMOtherm calculations employing C1.2, release 01.02. They similarly found the ionic liquid-rich branch of the binodal shifted to a significantly lower alkanol concentration, and their calculated temperature for the UCST does not deviate much from the experimental results.

Marsh and co-workers varied the length of the alkyl substituent in the cation of the ionic liquid (from butyl to octyl) but used a single solvent (1-butanol) only. They found a better performance of COSMOtherm calculations, especially relating to the coordinates of the UCST, which were reproduced quite well. From our findings, we assume that COSMO-RS can predict the expected existence of an immiscibility region, which is endorsed by the fact that COSMOtherm calculations yielded no demixing for the system ([bmim][PF_6] + methanol) between (253 and 303) K, but quantitative calculations for liquid−liquid equilibrium are not yet accomplished satisfactorily.

Conclusions

Liquid−liquid equilibria for binary systems of the ionic liquid [bmim][PF_6] and three alkanols were investigated at temperatures from about (263 to 362) K using the (synthetic) cloud-point method and (analytical) UV spectroscopy. The UV technique enabled to map parts of the alkanol-rich branch of the binodal for the first time. All systems exhibit liquid−liquid equilibria with a UCST behavior, and the spread of a biphasic regime is strongly determined by the molecular size of the alkanol. A change from ethanol for 1-butanol leads to expansion of the miscibility gap accompanied by a raise in the UCST. With respect to process design (e.g., liquid−liquid extraction in the presence of an ionic liquid), shrinking or broadening of the demixing region is an important aspect and quite easily tunable by a modification of the solvent.

The experimental data were correlated applying the UNIQUAC model and compared to predictions from the quantum chemical COSMO-RS method. COSMO-RS is able to predict such liquid−liquid equilibrium, but strictly interpreted, a reliable predictive mapping of the binodal curves was not yet possible.

Acknowledgment

We acknowledge Dr. K. Massonne and Dr. O. Huttenloch from BASF AG, Ludwigshafen, Germany, for providing ionic liquid samples and Dr. M. Diedenhofen from COSMOlogic GmbH & Co. KG, Leverkusen, Germany, for the COSMOtherm calculations employing C1.2, release 05.02 shown in Figure 7. We also thank Prof. K. N. Marsh, Department of Chemical & Process Engineering, University of Canterbury, Christchurch, New Zealand, for providing the Master Thesis of C.-T. Wu.

Literature Cited

(1) Maase, M. Erstes technisches Verfahren mit ionischen Flüssigkeiten. *Chem. Unserer Zeit* **2004**, *38*, 434−435.
(2) Maase, M.; Massonne, K.; Halbritter, K.; Noe, R.; Bartsch, M.; Siegel, W.; Stegmann, V.; Flores, M.; Huttenloch, O.; Becker, M. Method for the separation of acids from chemical reaction mixtures by means of ionic fluids. World Patent WO 03/062171, July 31, 2003.
(3) Swatloski, R. P.; Holbrey, J. D.; Rogers, R. D. Ionic liquids are not always green: hydrolysis of 1-butyl-3-methylimidazolium hexafluorophosphate. *Green Chem.* **2003**, *5*, 361−363.

(4) Swatloski, R. P.; Visser, A. E.; Reichert, W. M.; Broker, G. A.; Farina, L. M.; Holbrey, J. D.; Rogers, R. D. Solvation of 1-butyl-3-methylimidazolium hexafluorophosphate in aqueous ethanol—a green solution for dissolving 'hydrophobic' ionic liquids. *Chem. Commun.* **2001**, 2070−2071.
(5) Swatloski, R. P.; Visser, A. E.; Reichert, W. M.; Broker, G. A.; Farina, L. M.; Holbrey, J. D.; Rogers, R. D. On the solubilization of water with ethanol in hydrophobic hexafluorophosphate ionic liquids. *Green Chem.* **2002**, *4*, 81−87.
(6) Marsh, K. N.; Deev, A.; Wu, C.-T.; Tran, E.; Klamt, A. Room temperature ionic liquids as replacements for conventional solvents−a review. *Korean J. Chem. Eng.* **2002**, *19*, 357−362. The results of this paper are drawn from the Master Thesis by C.-T. Wu (Thermophysical properties of room temperature ionic liquids and their mixtures, Master Thesis, University of Canterbury, Christchurch, New Zealand, 2003.)
(7) Najdanovic-Visak, V.; Esperança, J. M. S. S.; Rebelo, L. P. N.; Nunes da Ponte, M.; Guedes, H. J. R.; Seddon, K. R.; de Sousa, H. C.; Szydlowski, J. Phase behaviour of room temperature ionic liquid solutions: an unusually large co-solvent effect in (water + ethanol). *Phys. Chem. Chem. Phys.* **2002**, *4*, 1701−1703.
(8) Wu, C.-T.; Marsh, K. N.; Deev, A. V.; Boxall, J. A. Liquid−liquid equilibria of room temperature ionic liquids and butan-1-ol. *J. Chem. Eng. Data* **2003**, *48*, 486-491. The results are drawn from Wu's Thesis in ref 6.
(9) Wagner, M.; Stanga, O.; Schröer, W. Corresponding states analysis of the critical points in binary solutions of room temperature ionic liquids. *Phys. Chem. Chem. Phys.* **2003**, *5*, 3943−3950.
(10) Najdanovic-Visak, V.; Esperança, J. M. S. S.; Rebelo, L. P. N.; Nunes da Ponte, M.; Guedes, H. J. R.; Seddon, K. R.; de Sousa, H. C.; Szydlowski, J. Pressure, isotope, and water co-solvent effects in liquid−liquid equilibria of (ionic liquid + alcohol) systems. *J. Phys. Chem. B* **2003**, *107*, 12797−12807.
(11) Najdanovic-Visak, V.; Serbanovic, A.; Esperança, J. M. S. S.; Guedes, H. J. R.; Rebelo, L. P. N.; Nunes da Ponte, M. Supercritical carbon dioxide-induced phase changes in (ionic liquid, water and ethanol mixture) solutions: application to biphasic catalysis. *Chem. Phys. Chem.* **2003**, *4*, 520−522.
(12) Marsh, K. N.; Boxall, J. A.; Lichtenthaler, R. Room temperature ionic liquids and their mixtures—a review. *Fluid Phase Equilib.* **2004**, *219*, 93−98.
(13) Swatloski, R. P.; Holbrey, J. D.; Memon, S. B.; Caldwell, G. A.; Caldwell, K. A.; Rogers, R. D. Using *Caenorhabditis elegans* to probe toxicity of 1-alkyl-3-methylimidazolium chloride based ionic liquids. *Chem. Commun.* **2004**, 668−669.
(14) Eckert, F.; Klamt, A. *COSMOtherm*, Version C2.1, Release 01.04; COSMOlogic GmbH & Co. KG: Leverkusen, Germany, 2004.
(15) Klamt, A.; Eckert, F. COSMO-RS: a novel and efficient method for the a priori prediction of thermophysical data of liquids. *Fluid Phase Equilib.* **2000**, *172*, 43−72. Erratum to "COSMO-RS: a novel and efficient method for the a priori prediction of thermophysical data of liquids". *Fluid Phase Equilib.* **2003**, *205*, 357.
(16) Franke, R.; Krissmann, J.; Janowsky, R. Was darf der Verfahrensingenieur von COSMO-RS erwarten? *Chem. Ing. Tech.* **2002**, *74*, 85−89.
(17) Eckert, F.; Klamt, A. Fast solvent screening via quantum chemistry: COSMO-RS approach. *AIChE J.* **2002**, *48*, 369−385.
(18) Abrams, D. S.; Prausnitz, J. M. Statistical thermodynamics of liquid mixtures: A new expression for the excess Gibbs energy of partly or completely miscible systems. *AIChE J.* **1975**, *21*, 116−128.
(19) Pérez-Salado Kamps, Á.; Tuma, D.; Xia, J.; Maurer, G. Solubility of CO_2 in the ionic liquid [bmim][PF_6]. *J. Chem. Eng. Data* **2003**, *48*, 746−749.
(20) Heintz, A.; Lehmann, J. K.; Wertz, C. Thermodynamic properties of mixtures containing ionic liquids. 3. Liquid−liquid equilibria of binary mixtures of 1-ethyl-3-methylimidazolium bis(trifluoromethylsulfonyl)-imide with propan-1-ol, butan-1-ol, and pentan-1-ol. *J. Chem. Eng. Data* **2003**, *48*, 472−474.
(21) Anthony, J. L.; Maginn, E. J.; Brennecke, J. F. Solution thermodynamics of imidazolium-based ionic liquids and water. *J. Phys. Chem. B* **2001**, *105*, 10942−10949.
(22) Carda-Broch, S.; Berthod, A.; Armstrong, D. W. Solvent properties of the 1-butyl-3-methylimidazolium hexafluorophosphate ionic liquid. *Anal. Bioanal. Chem.* **2003**, *375*, 191−199.
(23) Tuma, D.; Wagner, B.; Schneider, G. M. High-pressure solubility measurement of solids in near- and supercritical fluids. In *Supercritical Fluids as Solvents and Reaction Media*; Brunner, G., Ed.; Elsevier: Amsterdam, 2004; pp 121−146.
(24) Huddleston, J. G.; Visser, A. E.; Reichert, W. M.; Willauer, H. D.; Broker, G. A.; Rogers, R. D. Characterization and comparison of hydrophilic and hydrophobic room temperature ionic liquid incorporating the imidazolium cation. *Green Chem.* **2001**, *3*, 156−164.
(25) Heintz, A.; Lehmann, J. K.; Wertz, C.; Jacquemin, J. Thermodynamic properties of mixtures containing ionic liquids. 4. LLE of binary mixtures of [C_2MIM][NTf_2] with propan-1-ol, butan-1-ol, and pentan-1-ol and [C_4MIM][NTf_2] with cyclohexanol and 1,2-hexanediol including studies of the influence of small amounts of water. *J. Chem. Eng. Data* **2005**, *50*, 956−960.
(26) Domańska, U.; Marciniak, A. Solubility of 1-alkyl-3-methylimidazolium hexafluorophosphate in hydrocarbons. *J. Chem. Eng. Data* **2003**, *48*, 451−456.
(27) Crosthwaite, J. M.; Aki, S. N. V. K.; Maginn, E. J.; Brennecke, J. F. Liquid phase behavior of imidazolium-based ionic liquids with alcohols. *J. Phys. Chem. B* **2004**, *108*, 5113−5119.
(28) Scurto, A. M.; Aki, S. N. V. K.; Brennecke, J. F. CO_2 as a separation switch for ionic liquid/organic mixtures. *J. Am. Chem. Soc.* **2002**, *124*, 10276−10277.
(29) Liu, Z.; Wu, W.; Han, B.; Dong, Z.; Zhao, G.; Wang, J.; Jiang, T.; Yang, G. Study on the phase behaviors, viscosities, and thermodynamic properties of CO_2/[C_4mim][PF_6]/methanol system at elevated pressures. *Chem. Eur. J.* **2003**, *9*, 3897−3903.
(30) Zhang, Z.; Wu, W.; Liu, Z.; Han, B.; Gao, H.; Jiang, T. A study of tri-phasic behavior of ionic liquid−methanol−CO_2 systems at elevated pressures. *Phys. Chem. Chem. Phys.* **2004**, *6*, 2352−2357.
(31) Bondi, A. *Physical Properties of Molecular Crystals, Liquids, and Glasses*; John Wiley & Sons: New York, 1968.
(32) Marcus, Y. *Ion Properties*; Dekker: New York, 1997.
(33) Klamt, A.; Schüürmann, G. COSMO: a new approach to dielectric screening in solvents with explicit expressions for the screening energy and its gradient. *J. Chem. Soc., Perkin Trans. 2* **1993**, 799−805.

Received for review November 8, 2005. Accepted May 23, 2006.

JE050474J